# Structurization and Visualization of Design Space by Fluid Informatics

Shigeru Obayashi (Professor), Jeong Shinkyu (Associate Professor), and Koji Shimoyama (Assistant Professor)

**Multi-Objective Design Exploration (MODE) is presented to address Multidisciplinary Design Optimization problems. MODE reveals the structure of the design space from the trade-off information and visualizes it as a panorama for Decision Maker. The present form of MODE consists of Kriging Model, Adaptive Range Multi Objective Genetic Algorithms, Analysis of Variance and Self-Organizing Map. The application to the regional jet design illustrates how the present approach finds design knowledge.**

## 1.1. Introduction

Multidisciplinary design optimization (MDO) is gaining great importance in aerospace engineering. A typical MDO problem involves multiple competing objectives. While single objective problems may have a unique optimal solution, multi-objective problems (MOPs) have a set of compromising solutions, largely known as the trade-off surface, Pareto-optimal solutions or non-dominated solutions. These solutions reveal trade-off information among different objectives. They are optimal in the sense that no other solutions in the search space are superior to them when all objectives are taken into consideration. A designer will be able to choose a final design with further considerations.

Evolutionary algorithms (EAs)[1] are suitable for finding many Pareto-optimal solutions. However, because EAs are population-based approaches, they generally require a large number of function evaluations. To alleviate the computational burden, the use of the response surface method (RSM) has been introduced as a surrogate model.[2] The surrogate model used in this study is the Kriging model.[3,4,5]

A MDO system denoted multi-objective design exploration (MODE) was proposed in Obayashi et al[6]. and is illustrated in Figure 1.1. MODE is not intended to provide an optimal solution. MODE reveals the structure of the design space from trade-off information and visualizes it as a panorama for a decision maker. The present form of MODE consists of the Kriging model, adaptive range multi objective genetic algorithms, analysis of variance and a self-organizing map (SOM).[7] SOM divides the design space into clusters. Each cluster represents a set of designs containing specific design features. A designer may find an interesting cluster with good design features. Such design features are composed of a combination of design variables. If a particular combination of design variables is identified as a sufficient condition belonging to a cluster of interest, it can be considered as a design rule. Rough set theory[8] and other data mining techniques have been employed to extract design rules. Through the applications of MODE, this article illustrates the importance of understanding the design problem better instead of obtaining a single optimal solution.

In Japan, the New Energy and Industrial Technology Development Organization (NEDO) subsidized the development of an environmentally friendly high performance small jet aircraft. Mitsubishi Heavy Industries, Ltd. (MHI) was the prime contractor for the project. The purpose of this project was to build a prototype aircraft using advanced technologies, such as low-drag wing design, and lightweight composite structures, which were necessary for the reduction of environmental burdens. In March 2008, MHI decided to bring this conceptual aircraft into commercial use. This commercial jet aircraft, named the Mitsubishi regional jet (MRJ), has a capacity of about 70-90 passengers. This project focused on environmental issues, such as reduction of exhaust emissions and noise. Moreover, in order to bring the jet to market, lower-cost development methods using computer-aided design were also employed in this project. This article discusses two applications of MODE: MDO for a regional-jet wing with engine-airframe and structural design optimization for a regional-jet horizontal tail.


Transdisciplinary Fluid Integration Research Center, Institute of Fluid Science, Tohoku University

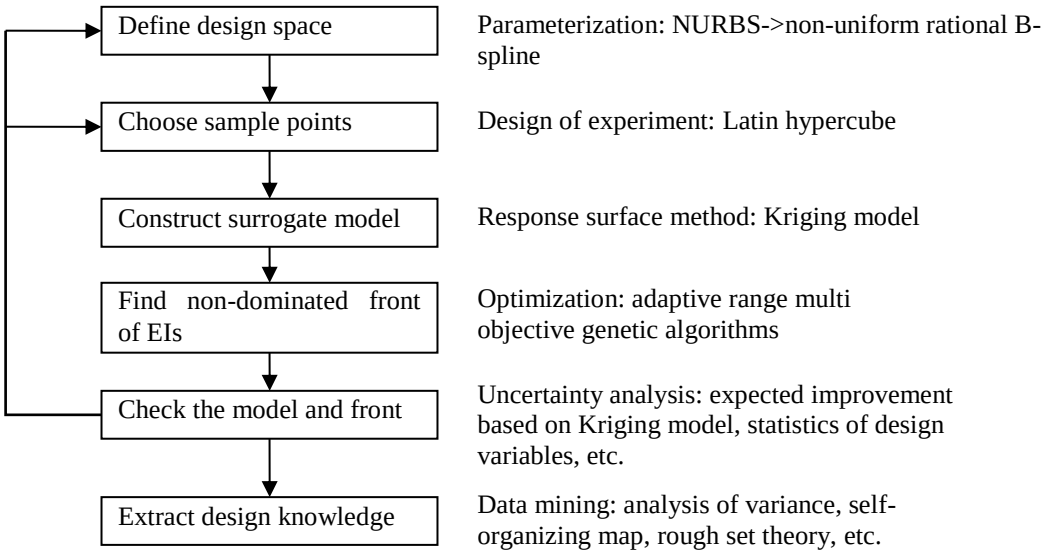


**Figure 1.1 Flowchart of multi-objective design exploration with component algorithms**

## 1.2. MDO SYSTEM

This MDO system consists of three modules: the mesh generation module, CFD & CSD module, and Kriging model & Optimization module.

### 1.2.A. Mesh Generation Module

In this study, NURBS[9,10] technique employing the B-spline function is adopted. A total number of the design variables is 26. This number was determined as results of comparisons with PARSEC.[11] Especially, NURBS has higher degree of freedom than PARSEC near the leading and trailing edges.

A speedy and robust surface mesh generation system which is applicable to engine-airframe integration is necessary. Although the unstructured dynamic mesh method is very useful for the modification of the wing shape,[12] this method sometimes produces the distorted mesh for a large displacement. Furthermore, In the case of the engine-airframe integration, this method cannot be applied because of complexities at junctions among wing, fuselage, pylon, and nacelle. In this study, wing-body-nacelle-pylon configuration mesh is automatically generated in the following steps (Figure 1.1).

(a) Airfoil sections are defined by NURBS specified by the design variables.
(b) 3D wing is generated using the airfoil sections.
(c) Extract the intersection lines among wing, fuselage, and nacelle-pylon.
(d) Delete the extra wing and pylon geometries which are inside of other geometies.
(e) Combine the wing, the body, and the nacelle-pylon.
(f) Specify mesh point distributions along ridge lines.
(g) Generate unstructured surface mesh using the advancing front method of TAS-Mesh.[13,14]
(h) Generate unstructured volume mesh using delaunay tetrahedral meshing.[15]

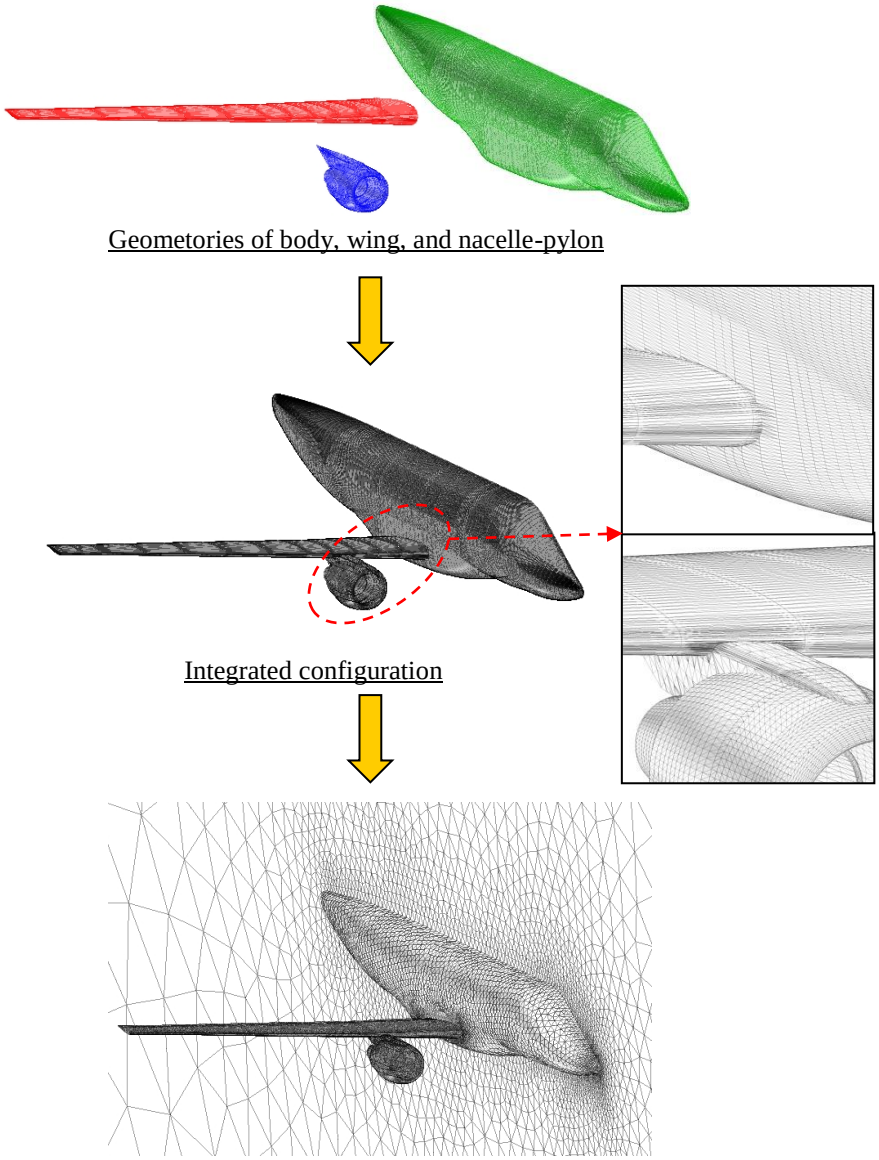


**Figure 1.2 Procedures for mesh generation**

### 1.2.B. CFD & CSD Module

In order to evaluate aerodynamic and structural performances, CFD&CSD module in Figure 1.2 is performed. The procedure is as follows:

(a) Euler analysis is performed for the sample points.
(b) Using the pressure distribution obtained from the Euler analysis, structural and flutter analysis models are generated by FLEXCFD which is an aeroelastic-structural interface code.
(c) Structural optimization is conducted to minimize wing weight under the strength and flutter constraints.

In the CFD&CSD module, structural optimization of a wing box is performed to realize minimum weight with constraints of strength and flutter. Given the wing outer mold line for each individual, the finite element model of wing box is generated automatically by the FEM generator for the structural optimization. The wing box model mainly consists of shell elements representing skin, spar and rib. Other wing components are modeled using concentrated mass elements. In the present study, MSC. NASTRAN[16] which is a high-fidelity commercial software is employed for the structural and aeroelastic evaluations.

### 1.2.C. Kriging Model & Optimization Module

Aerodynamic optimization using MOGA requires a tremendous computational time for objective function evaluations, even with a high performance supercomputer facility. To make the optimization more practical, an approximation model is introduced. The approximation model used in this study is the Kriging model.[17,18] This model, developed in the field of spatial statistics and geostatistics, predicts the distribution of function values at unknown points instead of the function values themselves. From the distribution of function values, both function values and their uncertainty at unknown points can be estimated. By using these values, the balanced local and global search is possible. This concept is expressed as the criterion 'Expected Improvement (EI)' [19] EI indicates the probability being superior to the current optimum in the design space. By selecting the maximum EI point as an additional sample point for the Kriging model, the improvement of the model accuracy and the exploration of the optimum can be achieved at the same time.

## 1.3. MDO FOR THE REGIONAL-JET WING WITH ENGINE-AIRFRAME INTEGRATION

Under the regional-jet project in Japan, Tohoku University participated as a collaborator and published a number of research results. Obayashi et al.[6] and Takenaka et al.[10] provided an overview of the collaborative works. Chiba et al.[20] and Kumano et al.[21] gave an account of the MDO system development for the main wing. Hatanaka et al.[22] and Kumano et al.[23] described the MDO system for engine-airframe integration. The winglet design was performed by Takenaka et al.[24] Aeroelastic simulations were also performed in the works provided by Kumano et al.[25] and Morino et al.[26]

### 1.3.A. Definition of optimization problem

The application shown here is the MDO tool for a regional-jet wing design with engine-airframe integration.[23] It should be noted that the optimized wing is not the exact MRJ wing; rather, the acquired design knowledge from the present application has been utilized for the MRJ wing design. Integration is an imperative issue in aircraft design. The shock wave generated inboard of the pylon may lead to flow separation and buffeting. To prevent these phenomena, the wing shape near the pylon has been optimized. The following design objectives are considered here.

<Objective functions>

Minimize

- Drag under cruising conditions (CD).
- Shock strength near wing-pylon junction (–Cp,max).
- Structural weight of the main wing (Wing weight).

<Design variables>

- Airfoil shapes of lower surface at 2 spanwise sections = 26 variables
- Twist angles at 4 sections = 4 variables

30 variables in total

<Constraints>

- Wing thickness > specified value
- Rear spar height > specified value
- Strength margin > specified value
- Flutter margin > specified value

### 1.3.B. Optimization results

During the optimization, the update of the Kriging models was performed six times. A total of 149 sample points were used. Figure 1.3 shows the performance of the baseline configuration and those of additional sample points at every iteration. As the iteration progressed, sample points moved toward the optimum direction indicating that the additional sample points for update were selected successfully. Several solutions with improvements in all objective function values compared with the baseline shape were obtained. One of the solutions was improved in 7.0 counts in CD, 0.503 in –Cp,max, and 21.6 kg in the wing weight compared with the performance of the baseline shape.

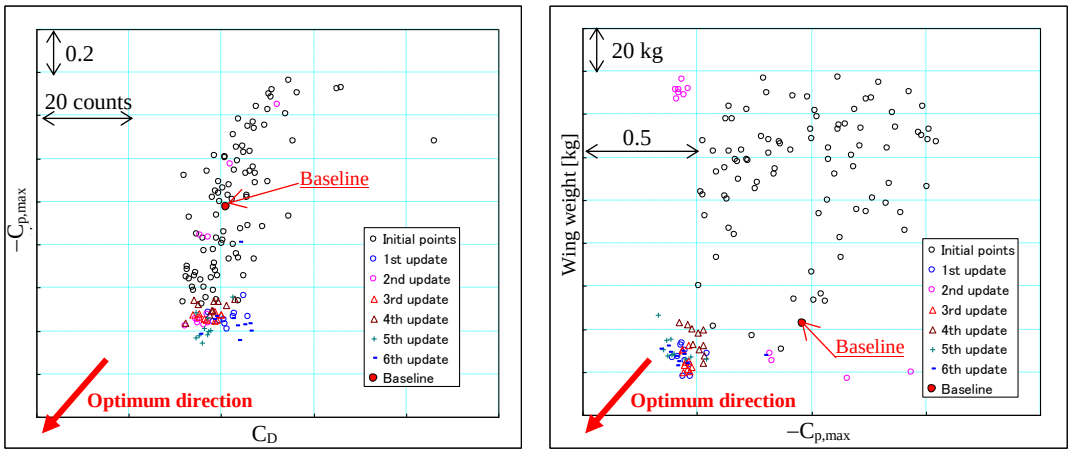


(a) $C_D$ - $-C_{p,max}$ (b) $-C_{p,max}$ - Wing weight

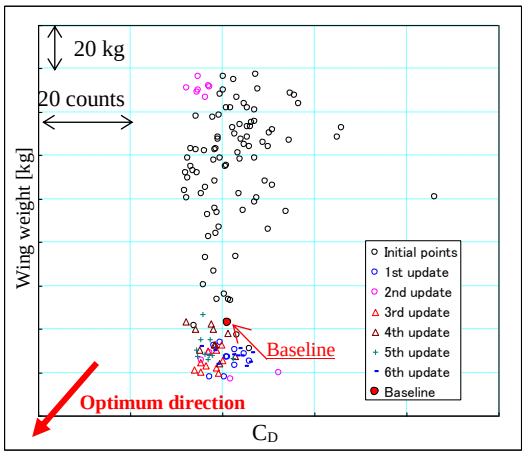


(c) $C_D$ - Wing weight

**Figure 1.3 Comparison of design performance among the baseline shape and sample points through Kriging updates**

### 1.3.C. Airfoil parameters used in data mining

Data mining was performed using airfoil parameters that differed from non-uniform rational B-spline (NURBS) design variables. The difference is due to the fact that NURBS control points have no aerodynamic or structural significance. Figure 1.4 shows the airfoil parameters of interest. XmaxL represents the distance from the leading edge to the maximum thickness point of the lower half of the airfoil. maxL is the corresponding maximum thickness of the lower half. XmaxTC is the distance from the leading edge to the maximum thickness point. maxTC is the corresponding maximum thickness. In addition, sparTC is the thickness at the front spar. These parameters are taken at two wing sections as shown in Table 1.1.

| Number | Airfoil parameters |
|---|---|
| dv1 | XmaxL @ η= 0.12 |
| dv2 | XmaxL @ η= 0.29 |
| dv3 | maxL @ η= 0.12 |

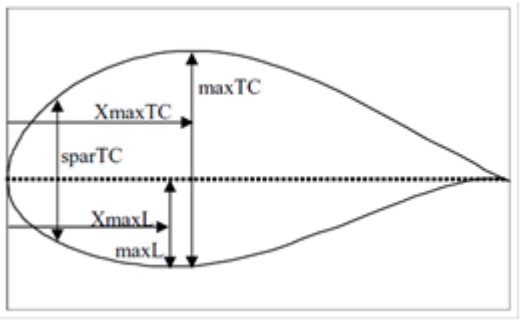


| | |
|---|---|
| dv4 | maxL @ η= 0.29 |
| dv5 | XmaxTC @ η= 0.12 |
| dv6 | XmaxTC @ η= 0.29 |
| dv7 | maxTC @ η= 0.12 |
| dv8 | maxTC @ η= 0.29 |
| dv9 | sparTC @ η= 0.12 |
| dv10 | sparTC @ η= 0.29 |

**Figure 1.4 Airfoil parameters used for data mining**

**Table 1.1 Airfoil parameters used for data mining**

ANOVA is a statistical data mining technique that reveals the effects of each design variable on the objective and the constraint functions.[4] ANOVA uses the variance of the model due to individual variables and pairs of variables (interactions) of the approximation function based on the Kriging model. By decomposing the total variance of the model into components due to main effects and interactions, the influences of individual variables and their pairs on the objective function can be calculated. Because the present Kriging model allows nonlinear approximation, ANOVA is sufficient for the present data mining.

Figure 1.5 shows the results of ANOVA for each objective function. According to the results, dv2, dv7, and dv9 largely influence CD. dv6, dv10, and dv2 largely influence $-C_{p,max}$. Furthermore, dv6, dv8, and dv2 largely influence wing weight.

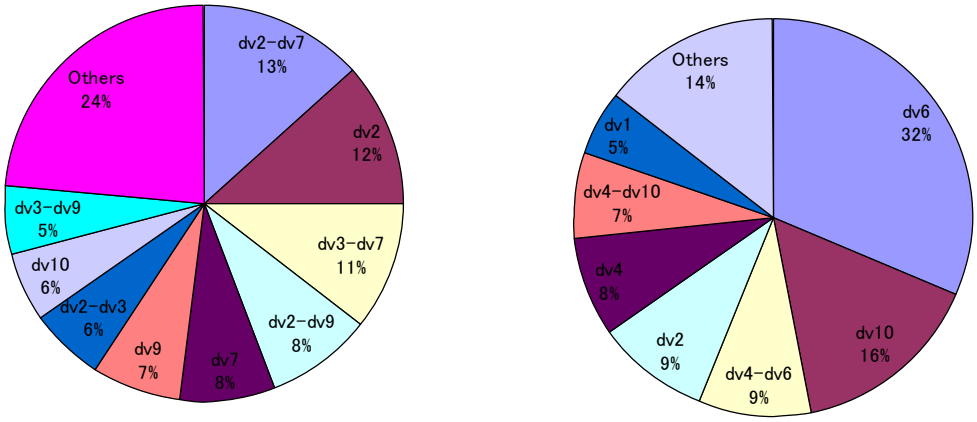


(a) $C_D$ (b) $-C_{p,max}$

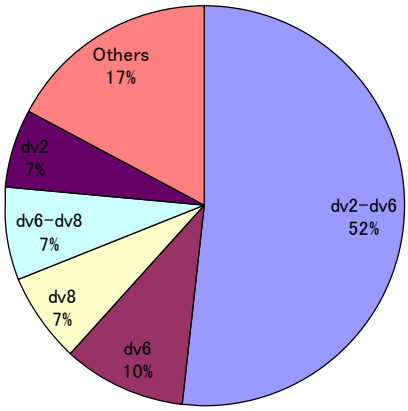


(c) Wing weight

**Figure 1.5 ANOVA results for each objective function based on airfoil parameters**

### 1.3.D. Visualization of design space

In order to visualize the design space, SOMs proposed by Kohonen[7] were employed. The following SOMs were generated by Viscovery SOMine (http://www.eudaptics.com/somine. accessed March 5, 2010). Once the user specifies the size of the map, this software automatically initializes the map based on the first two principal axes. The aspect ratio of the map is also determined according to the ratio of the corresponding principal components. The size of the map is usually 2000 neurons, which provides a reasonable resolution within a reasonable computational time.

Solutions uniformly sampled from the design space were projected onto the two-dimensional SOM. Figure 1.6 shows the resulting SOM with 12 clusters considering the three objectives. Furthermore, Figure 1.7 shows the same SOM colored by the three objectives. These color figures show that the SOM indicated in Figure 1.6 can be grouped as follows:

(a) The upper right corner corresponds to the designs containg heavy wing weight and low CD.
(b) The upper edge area corresponds to those with heavy wing weight.
(c) The lower right corner corresponds to those with low CD, –Cp,max, and light wing weight.
(d) The upper left corner corresponds to those with high CD.
(e) The lower left corner corresponds to those with high CD, and –Cp,max.

As a result, the lower right corner is the sweet spot in this design space, improving all three objective functions.

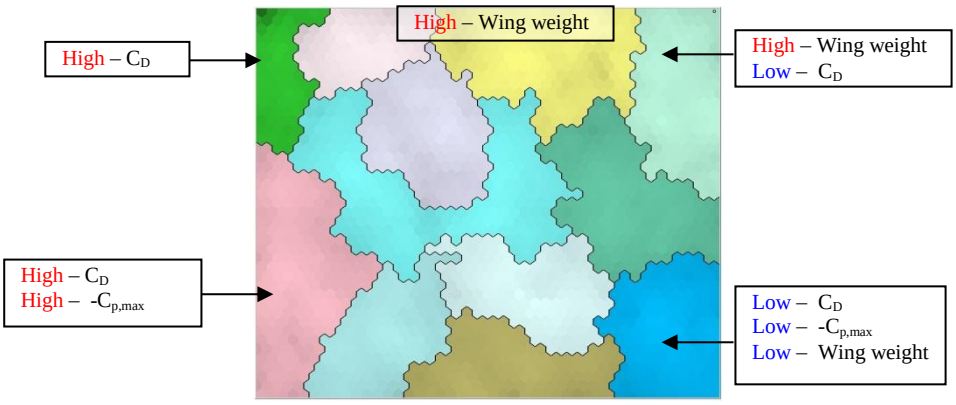


**Figure 1.6 Self-organizing map based on the design performance uniformly sampled from the design space**

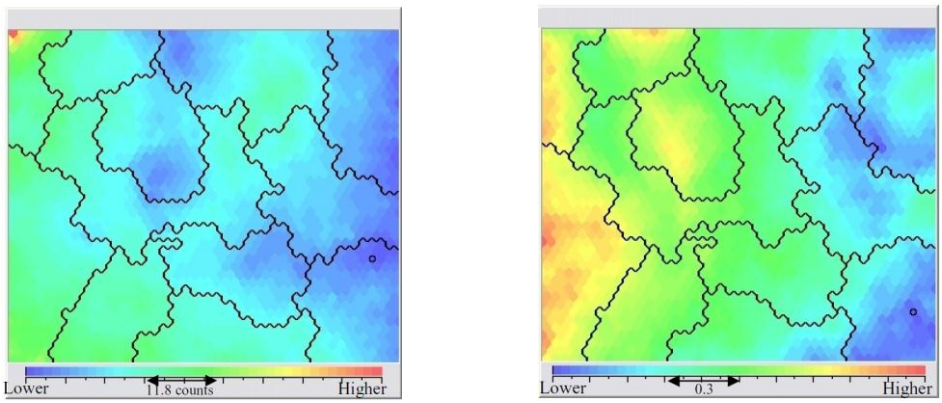


(a) CD (b) –Cp,max

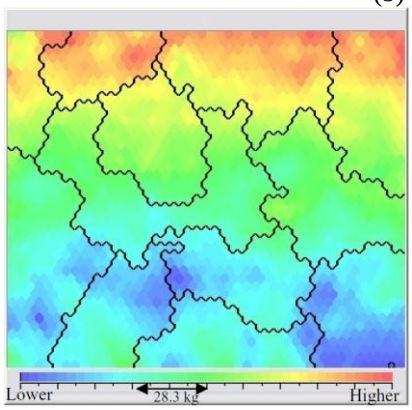


(c) Wing weight

**Figure 1.7 Self-organizing map based on the design performance colored by each objective function**

Figure 1.8 shows the same SOM colored by four airfoil parameters (dv2, dv6, dv7, and dv10, respectively). In Figure 1.8(a) colored by dv2, large dv2 values can be found at the right edge. This area corresponds to small CD and -Cp,max values as shown in Figure 1.7(a) and (b), respectively. This signifies that large dv2 values lead to acceptable CD and -Cp,max performance. Furthermore, in Figure 1.8(c) colored by dv7, low dv7 values can be found at the right edge. This color pattern is very similar to that for CD. This also indicates that low dv7 values lead to acceptable CD performance.

In Figure 1.8(b) colored by dv6, large dv6 values can be found at the right edge. This means that large dv6 values lead to good performance of –Cp,max. In addition, the color pattern of Figure 1.8(d) is very similar to that for –Cp,max. This means that low dv10 values lead to good performance of –Cp,max. As shown in Figure 1.9, large dv6 and low dv10 values mitigate the blockage between the wing and nacelle. Therefore, the shockwave between the wing and nacelle is weakened.

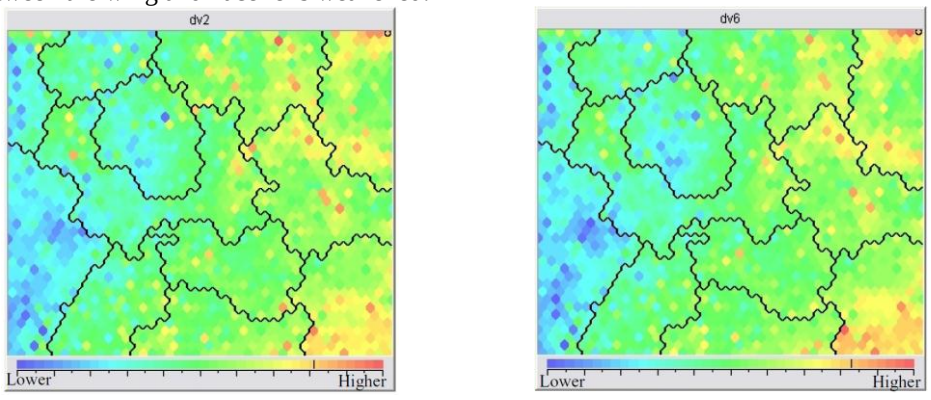


(a) dv2 (b) dv6

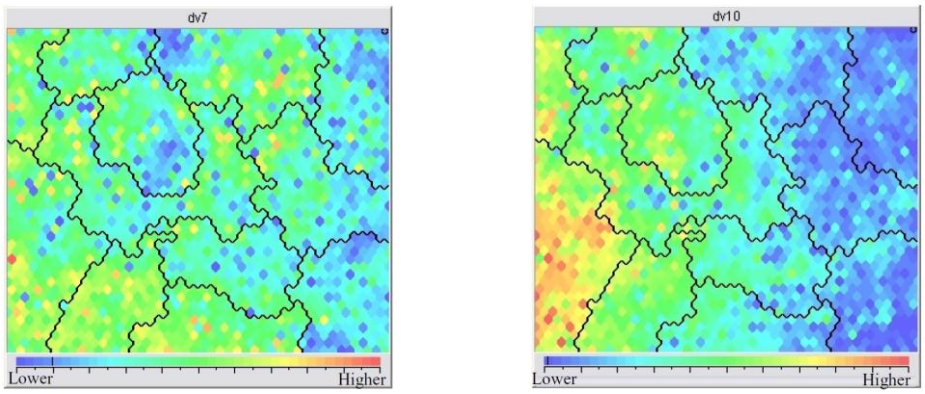


(c) dv7 (d) dv10

**Figure 1.8 Self-organizing map based on the design performance colored by the airfoil parameters**

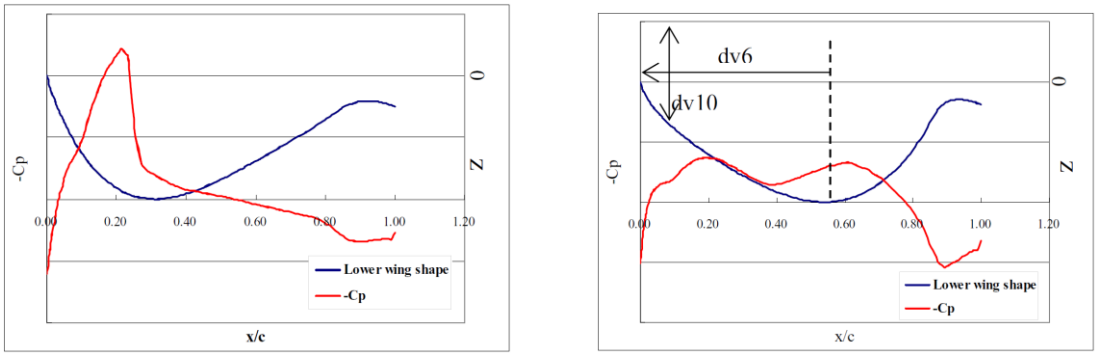


(a) High –Cp,max design (c) Low –Cp,max design

**Figure 1.9 Comparisons of airfoil lower surfaces and corresponding pressure distributions near the wing-pylon junction**

### 1.3.E. Extraction of design rules

Rough set theory was originally developed by Pawlak.[8] This mathematical method has been applied to human sense analysis because of its capability of handling ambiguous data and extracting underlying rules from that data. Because simulation data is deterministic, only the latter function was used. Rough set theory extracts design rules (decision rules) through the classification of set elements and set operations. Since details of the mathematical aspects of rough set theory can be found in the reference, the concept of applying rough set theory to an engineering design database are briefly explained: First, design samples with continuous variables are discretized to make logical set operation possible. Here, design variables are categorized into three levels. Each level is assigned to a different range of values of a design parameter and an objective function in such a way that the levels 1, 2 and 3 correspond to the minimum, middle and maximum ranges, respectively. For objective functions, clusters can be considered as a discrete category instead of these levels. Each design is then regarded as a deterministic rule describing conditions (design variables) and results (objective functions and clusters). Hence, all the data becomes a collection of rule sets. However, the rule sets still have as many conditions as the number of design variables, making it difficult for designers to understand them. Since some design variables do not affect the results or decisions, reducing the number of design variables required to obtain the same results is possible. This operation used for the purpose of obtaining minimum sets of conditions to determine the desired decision attributes is called 'reduct,' which makes obtaining simple rules with fewer conditions possible. Reduct is obtained from set operations. After obtaining reduced rule sets, the rule sets are filtered on the basis of the frequency to determine dominant rule sets. Finally, the meaning of the filtered rule sets is interpreted. Open software ROSSETA[27] was used for the necessary calculations.

The resulting rule appears, for example, 'dv1(medium) AND dv2(large) AND dv5(medium) AND dv7(medium) AND dv9(small) AND dv10(small) => Cluster(C6), occurrence(10).' It still appears complicated because the condition consists of a combination of five design parameters. In order to interpret the design rules more comprehensively, the frequency of appearance of small, medium and large for each design parameter was counted according to the sweet-spot cluster, small objective function values (CD,-Cp,max and wing weight), respectively, as summarized in Table 1.2. For example, dv2-sweet reads +9. This signifies that the condition

dv2(large) appears 9 times among the rules to belong to the sweet spot cluster. In other words, to belong to the sweet spot cluster, dv2, dv4 and dv6 should be large and dv9 and dv10 should be small.

The design knowledge discussed by using SOM in Section 3.3 can be summarized: a) Large dv2 improves CD and –Cp, b) Small dv7 improves CD, c) Large dv6 improves –Cp, d) Small dv10 improves –Cp.

Table 1.2 exhibits information consistent with these visualization results. Table 1.2, however, provides much more than the visualization. For example, dv4 should be large in order to belong to the sweet spot cluster, but it should be small in order to improve only the drag. Similarly, dv7 should be medium although it should be small in order to improve CD and –Cp. This illustrates the power of rough set theory. Visualization results depend on who looks at the figures and how deeply one reads. The result of rough set theory reduces oversights and reveals more detailed conditions.

| | Sweet | Cd | -Cp | WW |
|---|---|---|---|---|
| dv1 | 11 | 1 | +1 | 5 |
| dv2 | +9 | +2 | +6 | +3 |
| dv3 | 8 | -5 | 6 | 4 |
| dv4 | +10 | -3 | +5 | +11 |
| dv5 | 13 | +8 | +1 | 7 |
| dv6 | +7 | +6 | +3 | +3 |
| dv7 | 9 | -5 | -6 | 5 |
| dv8 | 2 | -4 | 3 | 2 |
| dv9 | -9 | -2 | -2 | -3 |
| dv10 | -14 | -9 | -8 | -8 |

**Table 1.2 Frequency of appearance in design rules (+ indicates large, - indicates small and no sign indicates medium)**

## 1.4. Conclusions

We discussed two applications of MODE: MDO for the regional-jet wing and structural design optimization for the regional-jet horizontal tail.

In the first application for the regional-jet wing MDO, ANOVA was first applied with the given set of design parameters for data mining. The results indicated which design parameters were influential. Next, visual data mining for the design space was performed using SOM. SOM divided the design space into clusters with specific design features. SOM obtained from the solutions uniformly sampled from the design space revealed that the sweet spot could exist. By comparing the SOM colored by influential design parameters found by ANOVA and the objective functions, several design rules were extracted. Finally, sufficient conditions belonging to the sweet spot cluster were extracted by rough set theory. Similarly sufficient conditions to improve each design objectives were extracted. The use of data mining will provide more knowledge about the design space and extract more information from the optimization problem.

## References


[1]Giannakoglou, K.C., "Design of optimal aerodynamic shapes using stochastic optimization methods and computational intelligence", *Progress in Aerospace Sciences*, 2002, 38, 43–76.

[2]Alexander I. J. Forrester, Andy J .Keane, "Recent advances in surrogate-based optimization" Progress in Aerospace Sciences, 2009, 45, 50–79.

[3]Jeong, S. and Obayashi, S., "Efficient Global Optimization (EGO) for multi-objective problem and data mining", IEEE Congress on Evolutionary Computation, Edinburgh, Scotland, 2005, pp. 2138-2145.

[4] Jones, D. R., Schonlau, M., and Welch, W. J., "Efficient Global Optimization of Expensive Black-Box Functions", Journal of Global Optimization, 1998, 13, 455-492.

[5]Keane, A. J., "Wing optimization using design of experiment, response surface, and data fusion methods", Journal of Aircraft, 2003, 40, 741-750.

[6]Obayashi, S., Jeong, S., and Chiba, K., "Multi-objective design exploration for aerodynamic configurations", 35th AIAA Fluid Dynamics Conference and Exhibit, 2005, pp. AIAA-2005-4666.

[7]Kohonen, T., Self-Organizing Maps. Berlin: Springer, 1995.

[8]Pawlak, Z.,Rough sets. International Journal of Computer & Information Sciences, 1982, 11, 341-356.

[9]Lepine, J., Guibault, F., Trepanier, J-Y., and Pepin, "Optimized Nonuniform Rational B-spline Geometrical Representation for Aerodynamic Design of Wings", AIAA Journal, 2001, Vol. 39, pp. 2033-2041.

[10]Takenaka, K., Obayashi, S., Nakahashi, K., Matsushima, K., "The Application of MDO Technologies to

the Design of a High Performance Small Jet Aircraft - Lessons learned and some practical concerns -", June 2005, AIAA paper 2005-4797.

[11]Oyama, A., Obayashi, S., Nakahashi, K., and Hirose, N., "Aerodynamic Wing Optimization via Evolutionary Algorithms Based on Structured Coding", Computational Fluid Dynamics Journal, 2000, Vol.8, No.4, pp. 570-577.

[12]Murayama, M., Nakahashi, K., and Matsushima, K., "Unstructured Dynamic Mesh for Large Movement and Deformation", 2002, AIAA Paper 2002-0122.

[13]Yamazaki, W., Matsushima, K., and Nakahashi, K., "Aerodynamic Optimization of NEXST-1 SST Model at Near-Sonic Regime," 2004, AIAA Paper 2004-0034.

[14]Ito, Y. and Nakahashi, K., "Direct Surface Triangulation Using Stereolithography Data," AIAA Journal, 2002, Vol. 40, No. 3, pp. 490–496.

[15]Sharov, D. and Nakahashi, K., "A Boundary Recovery Algorithm for Delaunay Tetrahedral Meshing", Proceedings of the 5th International Conference on Numerical Grid Generation in Computational Field Simulations, 1996, pp. 229–238.

[16]"MSC Software" website, URL: http://www.mscsoftware.com/.

[17] Jones, D. R., Schonlau, M., and Welch, W. J., "Efficient Global Optimization of Expensive Black-Box Function", Journal of global optimization, 1998, Vol.13, pp. 455-492.

[18]Jeong, S., Murayama, M., and Yamamoto, K., "Efficient Optimization Design Method Using Kriging Model", Journal of Aircraft, 2005, Vol.42, pp. 413-420.

[19]Matthias, S., "Computer Experiments and Global Optimization", Ph.D Dissertation, Statistic and Actuarial Science Dept., University of Waterloo, Waterloo, Ontario, 1997.

[20]Chiba, K., Oyama, A., Obayashi, S., Nakahashi, K., and Morino, H., "Multidisciplinary design optimization and data mining for transonic regional-jet wing", Journal of Aircraft, 2007, 44, 1100-1112.

[21]Kumano, T., Jeong, S., Obayashi, S., Ito, Y., Hatanaka, K., and Morino, H., "Multidisciplinary design optimization of wing shape for a small jet aircraft using kriging model", 44th AIAA Aerospace Sciences Meeting, Reno, NV, 2006, pp. 11158-11170.

[22]Hatanaka, K., Obayashi, S., and Jeong, S., "Application of the variable-fidelity MDO tools to a jet aircraft design", 25th International Congress of the Aeronautical Sciences, Hamburg, Germany, 2006.

[23]Kumano, T., Jeong, S., Obayashi, S., Ito, Y., Hatanaka, K., and Morino, H., "Multidisciplinary design optimization of wing shape with nacelle and pylon", European Conference on Computational Fluid Dynamics (ECCOMAS CFD 2006), Egmond aan Zee, The Netherlands ,2006.

[24]Takenaka, K., Hatanaka, K., Yamazaki, W., and Nakahashi, K., "Multidisciplinary design exploration for a winglet", Journal of Aircraft, 2008, 45, 1601-1611.

[25]Kumano, T., Morino, H., Jeong, S., and S., O., "Aeroelastic analysis using unstructured CFD method for realistic aircraft design", 8th World Congress on Computational Mechanics / 5th European Congress on Computational Methods in Applied Sciences and Engineering, Venice, Italy, 2008.

[26]Morino, H., Yamaguchi, H., Kumano, T., Jeong, S., and Obayashi, S., "Efficient aeroelastic analysis using unstructured CFD method and reduced-order unsteady aerodynamic model", 50th AIAA/ASME/ASCE/AHS/ASC Structures, Structural Dynamics, and Materials Conference, Palm Springs, CA, 2009, pp. AIAA 2009-2326.

[27]Øhrn, A., "ROSETTA Technical Reference Manual," Department of Computerand Information Science, Norwegian University of Science and Technology (NTNU), Trondheim, Norway, 2000.